Stochastic transition states: Reaction geometry amidst noise

Thomas Bartsch and T. Uzer
Center for Nonlinear Science and School of Physics, Georgia Institute of Technology, Atlanta, Georgia 30332-0430

Rigoberto Hernandez[a)]
Center for Nonlinear Science and School of Chemistry and Biochemistry, Georgia Institute of Technology, Atlanta, Georgia 30332-0300

(Received 7 July 2005; accepted 14 September 2005; published online 18 November 2005)

Classical transition state theory (TST) is the cornerstone of reaction-rate theory. It postulates a partition of phase space into reactant and product regions, which are separated by a dividing surface that reactive trajectories must cross. In order not to overestimate the reaction rate, the dynamics must be free of recrossings of the dividing surface. This no-recrossing rule is difficult (and sometimes impossible) to enforce, however, when a chemical reaction takes place in a fluctuating environment such as a liquid. High-accuracy approximations to the rate are well known when the solvent forces are treated using stochastic representations, though again, exact no-recrossing surfaces have not been available. To generalize the exact limit of TST to reactive systems driven by noise, we introduce a time-dependent dividing surface that is stochastically moving in phase space, such that it is crossed once and only once by each transition path. © *2005 American Institute of Physics*. [DOI: 10.1063/1.2109827]

I. INTRODUCTION

Transition state theory[1–7] (TST) plays a central role in chemistry because it provides both a tantalizingly simple approach to calculating chemical reaction rates and an intuitive interpretation of reaction mechanisms through the identification of the bottleneck between reactants and products. Although the rate could in principle be calculated exactly using known methods, in practice, it is often out of reach because such computations are laborious, even if quantum effects are ignored.[8–10] Therefore, the TST approximation to the rate has played a central role in kinetics, but its accuracy hinges on the optimal identification of the TS dividing surface.[11] Indeed TST is exact when the latter is crossed once and only once by each reactive trajectory.[7,12] While a constructive prescription for a no-recrossing TS dividing surface has long been sought, it was only in the 1970s that it was found in the special case of low-dimensional systems.[11,13,14] A general method that yields a no-recrossing TS dividing surface for reactions in arbitrarily many (but finite) degrees of freedom has been described only recently.[3,15–17] Nonetheless, even approximate TS dividing surfaces located near the phase-space bottlenecks between reactants and products provide a portrait of the activated complex that has been used routinely in the chemistry community.

Reactions in solution are even more complex because the presence of the solvent introduces a complicated many-body problem. Nevertheless, TST has been remarkably successful at providing accurate estimates of thermal reaction rates when a reasonable TS dividing surface can be identified.[18–21] Unfortunately, such estimates are seldom exact because the dividing surfaces available in the literature are not strictly free of recrossings. One approach lies in choosing the dividing surface so as to minimize the TST reaction rate.[12,22–25] The recrossing problem is thereby alleviated, but usually not eliminated. Alternatively, one can eliminate consideration of the nonreactive trajectories entirely by sampling the transition path ensemble (TPE) directly.[26–30] All such paths intersect the TS dividing surface and hence, as a collection, they provide a portrait of the activated complex. Using Monte Carlo approaches,[29,30] TPE can also be readily applied to complex molecular reactions in all-atom solvents, but it does not provide the simple geometric picture of a dividing surface free of recrossings.

The geometry of the finite-dimensional no-recrossing TS dividing surface is described in this paper for chemical reactions that can be represented using stochastic models of the solvent interactions. The moving TS dividing surface is most readily constructed in cases of uniform solvents such as those represented by the Langevin equation, as was summarized in a recent Letter.[31] The present article expands that discussion, and extends the results to the colored noise case of the generalized Langevin equation. It should be noted that a finite-dimensional-like TS dividing surface can be specified if an explicit infinite-dimensional model—viz., an infinite collection of harmonic oscillators—is used to represent the heat bath in the Langevin equation.[32–34] In spite of its simplicity, this model leads to an excellent approximation to the rate constant[32,35] that, remarkably, has been rederived without recourse to an explicit model of the heat bath.[36] Within the finite-dimensional phase space of the solute, the reaction geometry has also been illustrated using the stochastic separatrix (i.e., the collection of all phase-space points for which the reaction probability is 50%). That work portends the present development.[37]

In this paper, we introduce a generalized view of the

[a)]Electronic mail: hernandez@chemistry.gatech.edu

transition state that allows for the temporal variation of the solvent. While this has not yet been accomplished in an all-atom representation, we show here that if the solvent is modeled through the Langevin equation, a time-dependent TS dividing surface can be constructed that is strictly free of recrossings. This is achieved by identifying a privileged stochastic trajectory that remains in the vicinity of the barrier for all time. This transition-state trajectory serves as a moving origin to which geometric structures in a noiseless phase space, such as invariant manifolds and a no-recrossing surface,[3,16,17] are attached. The time-dependent dividing surface thus obtained adds to the evolving understanding of the geometric structures separating reactants from products in the presence of noise. The picture presented here provides a detailed time-resolved description of the reaction dynamics and, in particular, gives a precise geometric interpretation of the collective reaction coordinate introduced in Ref. 36.

The outline of the present paper is as follows: Sec. II recapitulates the macroscopic model of the solvent dynamics represented by the Langevin equation. In Sec. III, we introduce the fundamental construction that allows us to separate the full dynamics into the noisy TS trajectory and the noiseless relative motion. The TS trajectory for a particle driven by a white-noise bath is described explicitly in Sec. IV. The construction is simple and direct, and requires no more effort than that for a typical trajectory. Several statistical properties of the TS trajectory are also discussed in Sec. IV. In addition, the TS trajectory is used to compute reaction probabilities and the stochastic separatrix. The generalization of the TS trajectory to the chemically important case of colored noise is discussed in Sec. V.

II. PRELIMINARIES

The influence of the solvent on a chemical motion or reaction coordinate, $\mathbf{q}$, has been routinely represented using the Langevin equation (LE) of motion,[38,39]

$$\ddot{\mathbf{q}}_\alpha(t) = -\nabla_{\mathbf{q}} U(\mathbf{q}_\alpha(t)) - \boldsymbol{\Gamma}\dot{\mathbf{q}}_{\boldsymbol{\alpha}}(t) + \boldsymbol{\xi}_\alpha(t), \tag{1}$$

or the generalized Langevin equation (GLE) that allows for colored noise.[38–45] In Eq. (1), the vector $\mathbf{q}$ denotes a set of mass-weighted coordinates in a configuration space of arbitrary dimension N, $U(\mathbf{q})$ the potential of mean force governing the reaction, $\boldsymbol{\Gamma}$ a symmetric positive-definite friction matrix, and $\boldsymbol{\xi}_\alpha(t)$ a stochastic force. The subscript α here and throughout the paper labels a particular noise sequence $\xi_\alpha(t)$. For any given α, there are infinitely many different trajectories $\mathbf{q}_\alpha(t)$ that are distinguished by their initial conditions at some time t_0. Note that no restriction on the dimensionality of the configuration space is imposed and the derivations below work in one as well as in many dimensions. Although in Eq. (1) the deterministic force is formally assumed to be derived from a potential $U(\mathbf{q})$, it would be straightforward to include velocity-dependent forces from, e.g., a magnetic field.[46] Meanwhile, the stochastic force $\boldsymbol{\xi}_\alpha(t)$ is assumed to be Gaussian distributed with zero mean. It is related to the symmetric positive-definite friction matrix $\boldsymbol{\Gamma}$ through the fluctuation-dissipation theorem,[38,44,45,47,48]

$$\langle \boldsymbol{\xi}_\alpha(t)\boldsymbol{\xi}_\alpha^T(t')\rangle_\alpha = 2k_B T\boldsymbol{\Gamma}\,\delta(t-t'), \tag{2}$$

where the angular brackets denote the average over the instances α of the fluctuating force, and the Dirac δ function appears because white noise is local in time.

The assumption of white noise in Eq. (2) is consistent with the LE. It requires that the dynamics of the heat bath, which determines the correlation time of the fluctuating force, takes place on much shorter time scales than the dynamics along the chosen system coordinates—viz., the reaction coordinate and any other solute or solvent modes coupled to it. This is not always the case in applications relevant to chemistry where the dynamical time scales of the system and the bath are usually comparable. Nevertheless, the special case of white noise is treated in detail in the next two sections because it accommodates an explicit description of the relevant geometric structures. The generalization of the moving TS structures to the GLE is formally straightforward though mathematically more cumbersome. In the case of colored noise, the fluctuation-dissipation theorem requires that the friction kernel be nonlocal in time, viz., contain memory.[44,47,48] The TS trajectory is nevertheless computable and is presented in Sec. V. Perhaps surprisingly, geometric structures associated with the GLE are analogous to those in the LE.

A further assumption in this work requires that the reactant and product regions in configuration space are separated by a potential barrier, as is the case for most chemical reactions. The position of the barrier is marked by a saddle point $\mathbf{q}_0^\ddagger = 0$ of the potential $U(\mathbf{q})$. In the absence of noise, the saddle point is a fixed point of the dynamics. The invariant manifolds that determine the relevant phase-space geometry[3,16,17] are attached to it. In the presence of a fluctuating force, the geometric structures fixed at the saddle point no longer determine the reaction. As shown below, however, there is a unique stochastic trajectory $\mathbf{q}_\alpha^\ddagger(t)$ that can play the role of the saddle point and serve as the carrier of invariant manifolds.

Because the reaction rate is determined by the dynamics in a small neighborhood of the saddle point,[1,2] the deterministic force in the LE of Eq. (1) can be linearized around the saddle point to yield

$$\ddot{\mathbf{q}}_\alpha(t) = \boldsymbol{\Omega}\mathbf{q}_\alpha(t) - \boldsymbol{\Gamma}\dot{\mathbf{q}}_\alpha(t) + \boldsymbol{\xi}_\alpha(t), \tag{3}$$

where the first term in the right-hand side involves the symmetric force constant matrix,

$$\boldsymbol{\Omega}_{ij} = -\left.\frac{\partial^2 U}{\partial q_i \partial q_j}\right|_{\mathbf{q}=\mathbf{q}^\ddagger}. \tag{4}$$

Although any rectilinear coordinate system can be chosen, it is convenient to choose the one for which the force matrix,

$$\boldsymbol{\Omega} = \begin{pmatrix} \omega_b^2 & & & \\ & -\omega_2^2 & & \\ & & \ddots & \\ & & & -\omega_N^2 \end{pmatrix}, \tag{5}$$

is diagonal from the outset. In Eq. (3), q_1 is the reaction

coordinate, ω_b the barrier frequency, and $\omega_2, \ldots, \omega_N$ the frequencies of oscillations in the stable transverse normal modes $q_2, \ldots, q_N$.

III. THE FUNDAMENTAL CONSTRUCTION

The aim in the following is first to construct a no-recrossing surface for Eq. (3) and then to generalize the construction to correlated noise. It is well known that in the absence of noise and of dissipation—which are closely related by Eq. (2)—the phase-space hypersurface ($q_1=0$) is free of recrossings.[1,2,16,17] As shown below, the damping does not pose particular difficulties. The noise, however, does, because the fluctuating force leads the particle to move randomly back and forth, so that it will typically cross and recross any fixed dividing surface many times. We will overcome this difficulty by constructing a dividing surface that is itself randomly moving such as to avoid recrossing. To achieve this, the dividing surface must be constructed as a function of the fluctuating force.

Given any two trajectories $\mathbf{q}_\alpha(t)$ and $\mathbf{q}_\alpha^\ddagger(t)$ under the influence of the same fluctuating force, we define the relative coordinate,

$$\Delta\mathbf{q}(t) = \mathbf{q}_\alpha(t) - \mathbf{q}_\alpha^\ddagger(t). \tag{6}$$

It describes the location of the trajectory $\mathbf{q}_\alpha(t)$ with respect to the moving origin $\mathbf{q}_\alpha^\ddagger(t)$. By Eq. (3), the relative coordinate $\Delta\mathbf{q}(t)$ satisfies the deterministic equation of motion

$$\Delta\ddot{\mathbf{q}} = \boldsymbol{\Omega}\Delta\mathbf{q} - \boldsymbol{\Gamma}\Delta\dot{\mathbf{q}}, \tag{7}$$

and thus exhibits nonrandom noiseless dynamics. This result is indicated by the lack of a subscript α in $\Delta\mathbf{q}$. Due to the presence of the damping in Eq. (7), the dynamics of the relative coordinate, though noiseless, is still dissipative. Nevertheless, with respect to the relative dynamics, it is possible to specify a no-recrossing surface, as well as the invariant manifolds of the equilibrium point $\Delta\mathbf{q}=0$. These geometric objects in the noiseless phase space can be regarded as being attached to and propagating with the reference trajectory $\mathbf{q}_\alpha^\ddagger(t)$. They thus define moving invariant manifolds and a randomly moving no-recrossing surface in the phase space of the original, noisy system.

The relative dynamics between any two trajectories, $\mathbf{q}_\alpha(t)$ and $\mathbf{q}_\alpha^\ddagger(t)$, is described by Eq. (7). Because it is always noiseless, a moving no-recrossing surface can be thought of as attached to any reference trajectory. However, only a specific surface is relevant for the reaction dynamics: The crossing of the surface should indicate the transition of the trajectory $\mathbf{q}_\alpha(t)$ from the reactant to the product side of the barrier. It cannot serve that purpose if it is attached to a reference trajectory that is itself far away from the barrier. If the reference trajectory is chosen arbitrarily, it will typically descend into either the reactant or the product wells over time and thus lose its ability to carry a chemically meaningful dividing surface. Only a reference trajectory that remains in the vicinity of the barrier for all time without ever descending on either side of it can carry a no-recrossing surface that describes the reaction in the same way that a static dividing surface in conventional TST does. Indeed, we will show below that for each instance of the noise there is a unique reference trajectory with this property. This is the transition-state (TS) trajectory mentioned in the Introduction. We will henceforth restrict the notation $\mathbf{q}_\alpha^\ddagger(t)$ to this particular privileged reference trajectory.

The definition of the TS trajectory as "remaining close to the saddle point" for all time might at first appear somewhat vague. In the construction of the TS trajectory below, it will become clear that the exponential instability that is inherent in the noiseless dynamics associated with Eq. (3) in both the distant past and the remote future must be absent from the TS trajectory. A precise meaning can be given to the notion in statistical terms as follows: Because it is stochastic, at any given time there is a probability distribution for the TS trajectory in phase space. This distribution is invariant under the time evolution given by Eq. (3). In mathematical language, the TS trajectory represents an invariant measure of the noisy dynamical system.[49] That is, for any instance $\boldsymbol{\xi}_\alpha(\cdot)$ of the noise, where the dot indicates a function of time, there is an instance $\mathbf{q}_\alpha^\ddagger[\boldsymbol{\xi}_\alpha(\cdot)](t)$ of the TS trajectory that is given as a functional of the noise and is itself a function of time, t. It can be used to obtain the instance of the TS trajectory $\mathbf{q}_\alpha^\ddagger[\boldsymbol{\xi}_\alpha(\cdot)](t+\tau)$ that will be found if the origin from which time is measured is moved an increment $\tau\neq 0$. Alternatively, one can use the time-shifted noise $\boldsymbol{\xi}_\alpha(\cdot+\tau)$ and compute the corresponding TS trajectory $\mathbf{q}_\alpha^\ddagger[\boldsymbol{\xi}_\alpha(\cdot+\tau)](t)$. The TS trajectory is uniquely characterized by the requirement that these two ways of computing the time shift agree, $\mathbf{q}_\alpha^\ddagger[\boldsymbol{\xi}_\alpha(\cdot)](t+\tau) = \mathbf{q}_\alpha^\ddagger[\boldsymbol{\xi}_\alpha(\cdot+\tau)](t)$.

We have now given a general outline of the method. In the following sections, we will actually construct the TS trajectory, determine its statistical properties, and describe the invariant manifolds and the no-recrossing surface attached to it in detail.

IV. THE TRANSITION STATE IN WHITE NOISE

Equation (3) can be rewritten as a first-order equation of motion in the $2N$-dimensional phase space with the coordinates

$$\mathbf{z} = \begin{pmatrix} \mathbf{q} \\ \boldsymbol{v} \end{pmatrix}, \tag{8}$$

where $\boldsymbol{v}=\dot{\mathbf{q}}$, as

$$\dot{\mathbf{z}}_\alpha(t) = A\mathbf{z}_\alpha(t) + \begin{pmatrix} 0 \\ \boldsymbol{\xi}_\alpha(t) \end{pmatrix}, \tag{9}$$

with the $2N$-dimensional constant matrix

$$A = \begin{pmatrix} 0 & \boldsymbol{I} \\ \boldsymbol{\Omega} & -\boldsymbol{\Gamma} \end{pmatrix}, \tag{10}$$

where $\boldsymbol{I}$ is the $N\times N$ identity matrix. After diagonalizing the matrix A, its eigenvalues are denoted by ϵ_j and its corresponding eigenvectors by $\mathbf{V}_j$. The Langevin equation, Eq. (9), then decomposes into a set of $2N$-independent scalar equations of motion

$$\dot{z}_{\alpha j}(t) = \epsilon_j z_{\alpha j}(t) + \xi_{\alpha j}(t), \tag{11}$$

where $z_{\alpha j}$ are the components of $\mathbf{z}$ in the basis $\mathbf{V}_j$ of eigenvectors of A and $\xi_{\alpha j}$ the corresponding components of $[0, \boldsymbol{\xi}_\alpha(t)]^T$.

A. Relative dynamics

The noiseless equation of motion for the relative coordinate $\Delta\mathbf{q}(t)$ in Eq. (6), when lifted into phase space via Eq. (8) and expressed in diagonal coordinates, reads

$$\Delta\dot{z}_j(t) = \epsilon_j \Delta z_j(t). \tag{12}$$

It is solved by

$$\Delta z_j(t) = e^{\epsilon_j t}\Delta z_j(0), \tag{13}$$

with a set of integration constants $\Delta z_j(0)$. Equation (13) leads to a solution of the form

$$\Delta\mathbf{q}(t) = \sum_j c_j \boldsymbol{\nu}_j e^{\epsilon_j t}, \tag{14}$$

for the relative coordinate vector $\Delta\mathbf{q}(t)$, where $\boldsymbol{\nu}_j$ are the configuration-space parts of the phase-space eigenvectors $\mathbf{V}_j$ and the c_j are arbitrary constants. To identify reactive trajectories, one must consider the behavior of $\Delta\mathbf{q}(t)$ in the remote future and in the distant past and then determine those trajectories that pass across the barrier from the reactant to the product side.

The simplest case occurs in one degree of freedom where $\mathbf{\Omega}$ reduces to the squared barrier frequency ω_b^2 and $\mathbf{\Gamma}$ to a scalar damping coefficient γ. In this case, the matrix A can be diagonalized analytically. It possesses the eigenvalues

$$\epsilon_u = -\tfrac{1}{2}(\gamma - \sqrt{\gamma^2 + 4\omega_b^2}) > 0 \tag{15a}$$

and

$$\epsilon_s = -\tfrac{1}{2}(\gamma + \sqrt{\gamma^2 + 4\omega_b^2}) < 0, \tag{15b}$$

with the corresponding eigenvectors

$$\mathbf{V}_u = \begin{pmatrix} 1 \\ \epsilon_u \end{pmatrix} \text{ and } \mathbf{V}_s = \begin{pmatrix} 1 \\ \epsilon_s \end{pmatrix}. \tag{16}$$

The phase portrait of the dynamics is shown in Fig. 1(a). The eigenvectors corresponding to the positive and negative eigenvalues, respectively, span one-dimensional unstable and stable manifolds of the saddle point. They act as separatrices between reactive and nonreactive trajectories. The knowledge of the invariant manifolds allows one to determine the ultimate fate of a specific trajectory from its initial conditions. It should be clear that line, $\Delta q_u = 0$, in the quadrant of reactive trajectories acts as a surface of no recrossing.

In the absence of damping (and in units where $\omega_b = 1$), the invariant manifolds bisect the angles between the coordinate axes. The presence of damping destroys this symmetry. As the damping constant γ increases, on obtains the limits, $\epsilon_s \to 0$ and $\epsilon_u \to \infty$. Therefore, the unstable manifold rotates toward the q_u axis, and the stable manifold toward the $\dot{q}_u$ axis. In the limit of infinite damping, the invariant manifolds coincide with the axis. Thus, the fraction of phase space on the reactant side that corresponds to reactive trajectories decreases with increasing friction. This is intuitively clear because if the dissipation is strong, a trajectory must start at a given initial position with a high velocity to overcome the friction and cross the barrier.

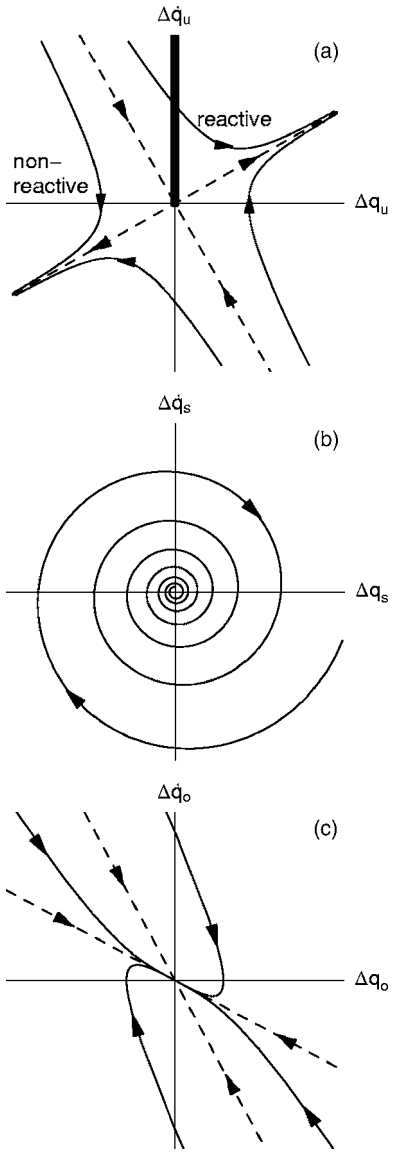

FIG. 1. Phase portrait of the noiseless damped dynamics corresponding to the linear Langevin equation (3) in (a) the unstable reactive degree of freedom, (b) a transverse stable degree of freedom, and (c) an overdamped transverse degree of freedom.

In multiple dimensions, the dynamics of the single unstable degree of freedom is the same as in the one-dimensional case shown in Fig. 1(a). Transverse damped oscillations, as shown in Fig. 1(b), must be added to this picture. Their presence manifests itself, for small damping, through $N-1$ complex conjugate pairs of eigenvalues ϵ_j. For stronger damping, some of the transverse modes can become overdamped, as illustrated in Fig. 1(c), so that further eigenvalues become real and negative. In any case, there is exactly one unstable eigenvalue with a positive real part. This eigenvalue is actually real and corresponds to the system sliding down the barrier. In all other directions, the dynamics is stable, and at least one eigenvalue is negative real. The dy-

namics in the distant past is determined by the eigenvalue or pair of eigenvalues with the largest negative real part.

The eigenvector corresponding to the most stable eigenvalue together with the unstable eigenvector span a plane in phase space in which the dynamics is given by the phase portrait of Fig. 1(a). Because the dynamics in all other, "transverse" directions is stable, the separatrices between reactive and nonreactive trajectories that we identified for the one-dimensional dynamics together with the transverse subspace form separatrices in the high-dimensional phase space. In a similar manner, a no-recrossing curve in the plane together with the transverse directions form a no-recrossing surface in the full phase space.

If the most stable eigenvalues occur as a complex conjugate pair, the leading dynamics in the remote past is given by an oscillation across the barrier that, because it is strongly damped, has a huge amplitude in the distant past and causes the system to cross the barrier infinitely often. This behavior is clearly unphysical. In fact, once the oscillations become large, nonlinearities of the reaction dynamics become relevant, and the ultimate fate of the trajectory can no longer be determined from the linear approximation. This situation can only occur if the damping is strong and at the same time the undamped transverse frequencies are so large that the corresponding eigenmodes do not become overdamped. This rare situation is ignored below.

An exception to the discussion above occurs if for any eigenvector $\boldsymbol{v}_j$ the component $v_j^{(1)}$ in the direction of the reaction coordinate is zero. In this case the excitation of the corresponding eigenmode has no impact on whether a trajectory is reactive or nonreactive. The unstable and the most stable eigenvalues must then be chosen among the eigenvalues with $v_j^{(1)} \neq 0$, which we call the "relevant" eigenvalues. Because the unstable eigenmode corresponds to the particle sliding down the barrier, it is always relevant. Similarly, there must be one relevant negative eigenvalue corresponding to the particle being shot at the barrier from infinity and coming to rest on it. The occurrence of irrelevant eigenvalues might seem a rather unlikely exception, but it does arise in the important special case of isotropic friction, where the friction coefficient $\boldsymbol{\Gamma} = \gamma \boldsymbol{I}$ is a scalar multiple of the identity matrix. In this situation, the friction does not couple different normal modes of the undamped dynamics, and all but two eigenvalues are irrelevant. In particular, our construction of a no-recrossing surface can always be carried out for isotropic friction.

B. The transition-state trajectory

The influence of noise in the equation of motion, Eq. (11), can be accounted for by means of the retarded Green's function

$$G^{\mathrm{ret}}(t) = \begin{cases} 0 & \text{if } t < 0 \\ e^{\epsilon_j t} & \text{if } t > 0, \end{cases} \tag{17}$$

which satisfies

$$\dot{G}^{\mathrm{ret}}(t) - \epsilon_j G^{\mathrm{ret}}(t) = \delta(t). \tag{18}$$

It gives the general solution of Eq. (11) as

$$z_{\alpha j}(t) = c_{\alpha j} e^{\epsilon_j t} + \int_{-\infty}^{\infty} G^{\mathrm{ret}}(t-\tau)\xi_{\alpha j}(\tau)d\tau$$

$$= c_{\alpha j} e^{\epsilon_j t} + \int_{-\infty}^{t} e^{\epsilon_j (t-\tau)}\xi_{\alpha j}(\tau)d\tau, \tag{19}$$

with arbitrary constants $c_{\alpha j}$. The integral

$$z_{\alpha j}^{\ddagger}(t) = \int_{-\infty}^{t} e^{\epsilon_j (t-\tau)}\xi_{\alpha j}(\tau)d\tau = \int_{-\infty}^{0} e^{-\epsilon_j \tau}\xi_{\alpha j}(t+\tau)d\tau \tag{20}$$

exists with probability one if $\mathrm{Re}\,\epsilon_j < 0$, i.e., for the stable components. Only for those, therefore, is the solution, Eq. (19), meaningful.

The first term in Eq. (19) tends to zero as $t \to \infty$, but it diverges exponentially as $t \to -\infty$. The only solution to Eq. (11) that remains bounded in the remote past is obtained by setting $c_{\alpha j} = 0$. But the TS trajectory has been defined as the unique trajectory that remains in the neighborhood of the saddle point at all times. It now becomes clear that this condition indeed determines the stable components of the TS trajectory uniquely and that they are given by Eq. (20). Because they depend on the noise $\xi_{\alpha j}(\cdot)$, the $z_{\alpha j}^{\ddagger}(t)$ are stochastic functions of time. From the second form given in Eq. (20), it should be obvious that the probability distribution of $z_{\alpha j}^{\ddagger}$ is stationary in time if the distribution of $\boldsymbol{\xi}_{\alpha}(\cdot)$ is itself stationary.

The solution in Eq. (19) fails for the unstable component of the trajectory, where $\mathrm{Re}\,\epsilon_j > 0$. To compute that component, we use the advanced Green's function

$$G^{\mathrm{adv}}(t) = \begin{cases} -e^{\epsilon_j t} & \text{if } t < 0 \\ 0 & \text{if } t > 0, \end{cases} \tag{21}$$

to obtain the solution

$$z_j(t) = c_{\alpha j} e^{\epsilon_j t} + z_{\alpha j}^{\ddagger}(t), \tag{22}$$

with constants $c_{\alpha j}$ and

$$z_{\alpha j}^{\ddagger}(t) = -\int_{t}^{\infty} e^{\epsilon_j (t-\tau)}\xi_{\alpha j}(\tau)d\tau = -\int_{0}^{\infty} e^{-\epsilon_j \tau}\xi_{\alpha j}(t+\tau)d\tau. \tag{23}$$

The position in Eq. (22) is bounded in the remote future only if $c_{\alpha j} = 0$. Therefore, $z_{\alpha j}^{\ddagger}(t)$ given in Eq. (23) can be identified as the component of the TS trajectory in the unstable direction. Notice that the stable components in Eq. (20) at time t depend on the past of the fluctuating force, whereas the unstable component in Eq. (23) depends on its future.

Through Eqs. (20) and (23), all components of the TS trajectory $\mathbf{z}_{\alpha}^{\ddagger}(t)$ in phase space have been specified. The TS trajectory $\mathbf{q}_{\alpha}^{\ddagger}(t)$ in configuration space can be obtained because the transformation connecting the position-velocity coordinates and diagonal coordinates is known. The consistency of the calculation can then be checked by verifying that the velocity obtained from the coordinate transformation is actually the time derivative of the position coordinate.

A specific instance of the TS trajectory for a system with two degrees of freedom (and a four-dimensional phase space) is shown in Fig. 2. It can be observed how the trajec-

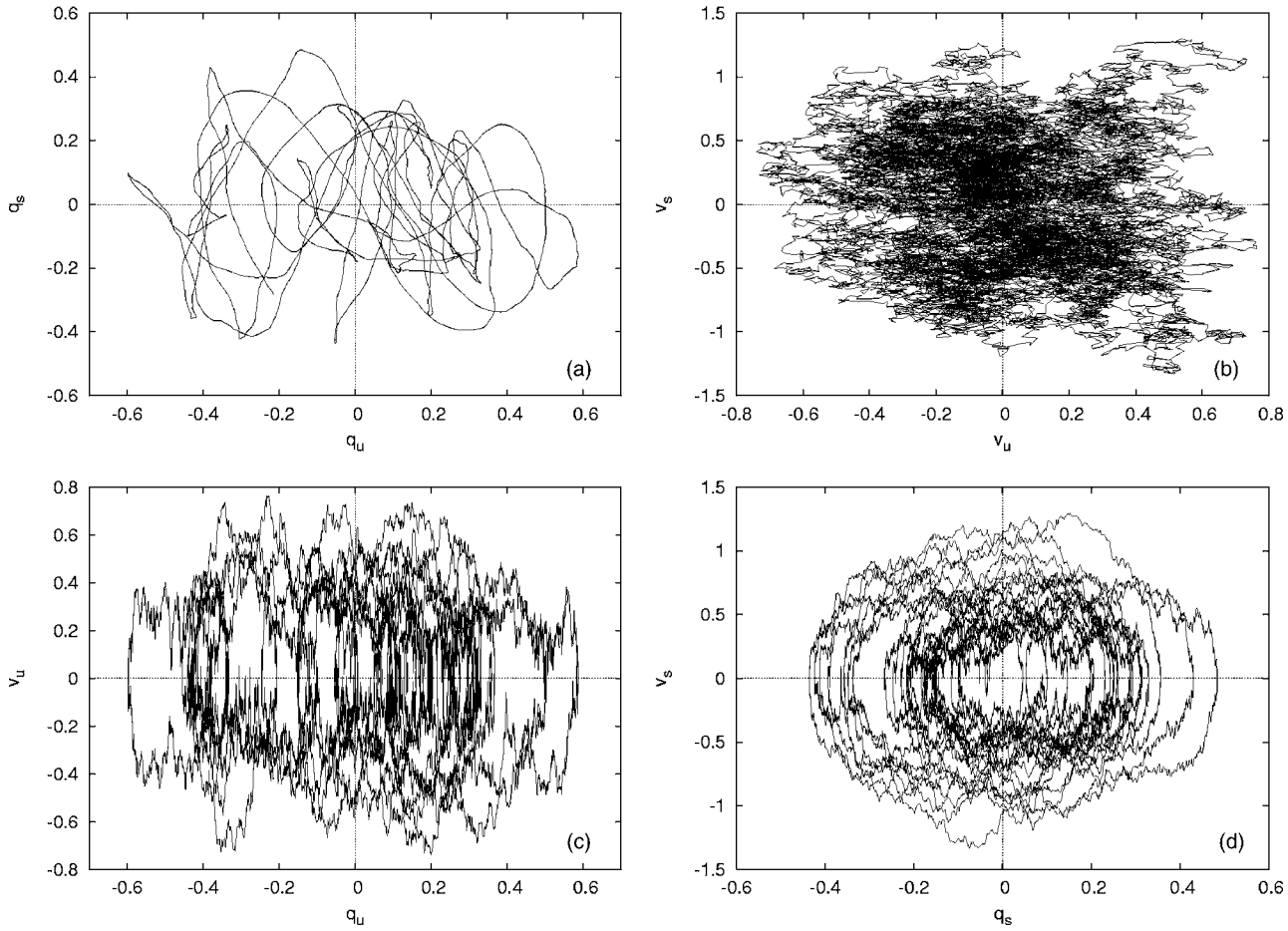

FIG. 2. A random instance of the TS trajectory in a system with $N=2$ degrees of freedom, projected onto (a) configuration space, (b) velocity space, (c) the reactive degree of freedom, and (d) the transverse degree of freedom. Units have been chosen so that $\omega_b=1$, $k_BT=1$. The transverse frequency is $\omega_2=2$, and friction is isotropic, $\mathbf{\Gamma}=\gamma\boldsymbol{I}$ with $\gamma=0.5$.

tory randomly wanders around in the vicinity of the saddle point without ever leaving it. The velocity space projection of the TS trajectory appears much more noisy than its configuration-space projection. This results because the environment is assumed to cause a fluctuating force in Eq. (1) that couples directly only to the velocity, but not to the position. It should be clear from the above discussion, however, that this condition can easily be relaxed. In the absence of noise and of damping, any trajectory would exhibit an elliptical orbit in the projection onto the stable degree of freedom This behavior is still visible in the noisy situation of Fig. 2(d) where a slow change of energy, corresponding to the size of the ellipse, is superimposed over the elliptic motion.

As described in Sec. III, the TS trajectory serves as the origin of a moving coordinate system, and the geometric structures in the noiseless phase space that we have described in Sec. IV A are attached to it. This is illustrated in Fig. 3 for two degrees of freedom. This case already exhibits all salient features of the dynamics in arbitrary high dimensions. The figure compares a specific instance of the TS trajectory with a transition path under the influence of the same noise. It can be seen how the transition path approaches the TS trajectory from the reactant side, remains in its vicinity for a while, and then wanders off to the product side. Because the moving invariant manifolds of the TS trajectory are known, it can be predicted already at time $t=0$ that the trajectory actually will lead to a reaction instead of returning to the reagent side of the saddle. From both the time-dependent plots and the time-independent projections in Figs. 3(a) and 3(c) it is clear that the transition path crosses the space-fixed TS surface $q_u=q_u^{\ddagger}=0$ several times before it finally descends on the product side. The moving TS surface $\Delta q_u=0$, by contrast, is crossed only once, at the reaction time $t_{\mathrm{react}}=8.500$. That this is actually the case can be seen from the curves in the top faces of each column, which indicate the noiseless relative motion $\Delta q(t)$, $\Delta v(t)$ between the TS trajectory and the transition path. In the relative coordinates we find, as expected, the hyperbolic motion known from Fig. 1 in the unstable degree of freedom, a damped oscillation in the stable transverse degree of freedom, and a superposition of the two in the configuration space projection in Fig. 3(c).

C. Statistical properties of the TS trajectory

If the noise $\xi_\alpha(t)$ is assumed to be Gaussian with zero mean, it is clear from Eqs. (22) and (23) that the same is true for all components $z_{\alpha j}^{\ddagger}$ of the TS trajectory and, by extension, also for its position and velocity coordinates. To specify their

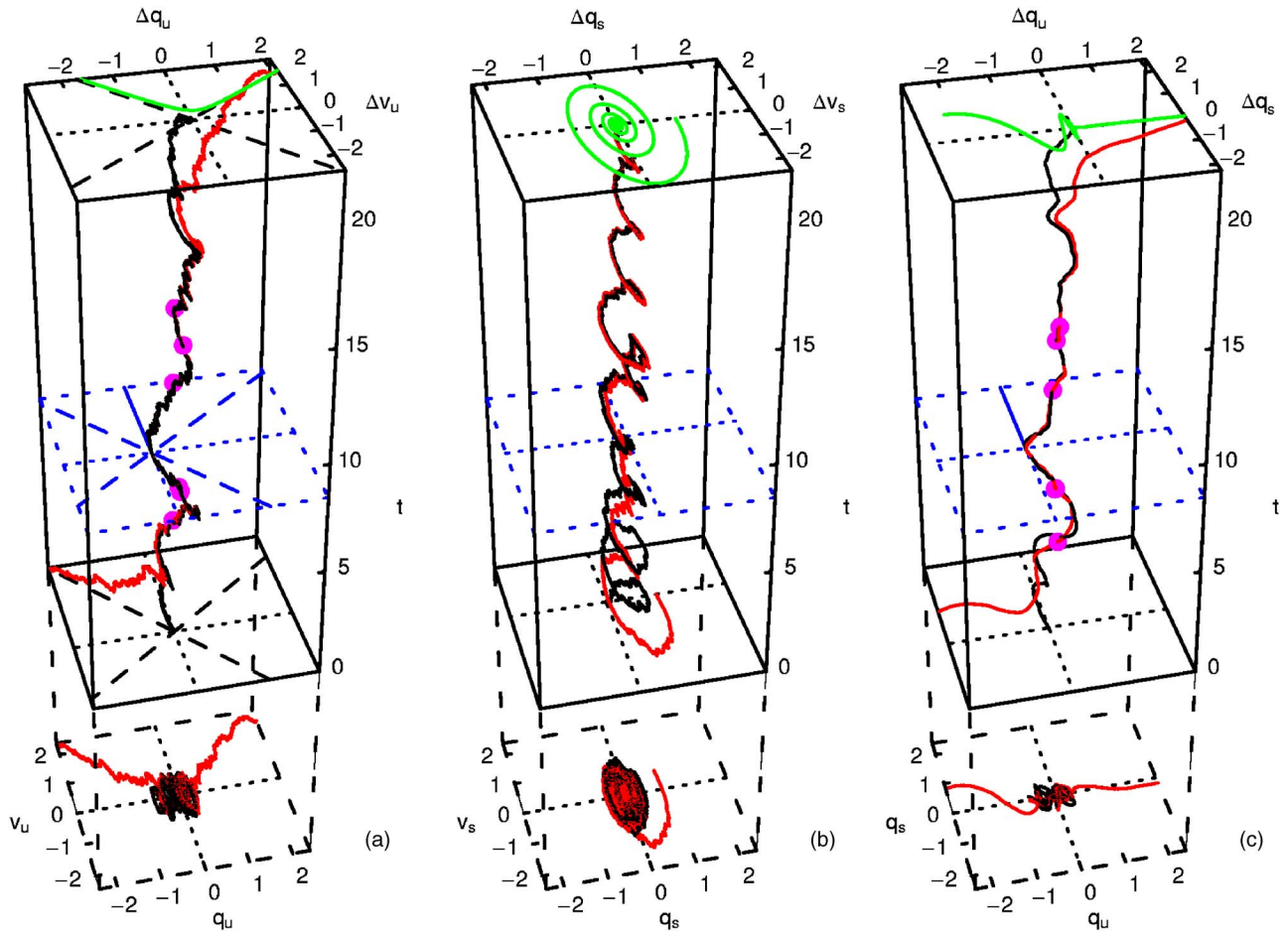

FIG. 3. The instance of the TS trajectory shown in Fig. 2 and a transition path under the influence of the same noise. Trajectories are projected onto (a) the reactive degree of freedom, (b) the transverse degree of freedom, and (c) configuration space. At the lower end of each column is a projection into the corresponding phase-space plane, disregarding time. The instantaneous positions of the moving coordinate axes (dotted) and, in (a), of the invariant manifolds (dashed) are shown at $t=0$, at $t=22$, and at the unique reaction time $t_{\mathrm{react}}=8.500$ where the TS is crossed. The solid line at t_{react} indicates the moving TS. The curves in the top faces of each panel illustrates the dynamics of the transition path in relative coordinates Δq, Δv [not to scale in (a), for graphical reasons].

joint probability distribution completely, it thus remains to calculate their time autocorrelation and cross-correlation functions.

The most general fluctuating force $\boldsymbol{\xi}_\alpha(t)$ satisfying the fluctuation-dissipation theorem, Eq. (2), can be written as

$$\boldsymbol{\xi}_\alpha(t) = \boldsymbol{g}\mathbf{W}_\alpha(t), \tag{24}$$

in terms of M realizations of standard white noise $\mathbf{W}_\alpha(t) = (W_{\alpha 1}(t), \ldots, W_{\alpha M}(t))^T$ normalized to

$$\langle W_{\alpha i}(t) W_{\alpha j}(s)\rangle_\alpha = \delta(t-s)\delta_{ij}, \tag{25}$$

and an $N \times M$ matrix g of coupling strengths satisfying

$$\boldsymbol{g}\boldsymbol{g}^{\mathrm{T}} = 2k_{\mathrm{B}}T\boldsymbol{\Gamma}. \tag{26}$$

The statistical properties of the noise are completely specified by Eq. (26). If $M > N$, a representation can be found that has fewer independent noise sources, but still satisfies Eq. (26) with the same matrix $\boldsymbol{\Gamma}$. For that reason, it can be assumed without loss of generality that $M \leqslant N$. The components of the noise in diagonal coordinates can be written as

$$\xi_{\alpha j}(t) = \sum_i \kappa_{ji} W_{\alpha i}(t), \tag{27}$$

with a set of constants κ_{ji} computed from the matrix $\boldsymbol{g}$ and the coordinate transform between position-velocity coordinates and diagonal coordinates.

With the noise term, Eq. (27), the time correlation function of two stable components (20) of the TS trajectory, with $\mathrm{Re}\,\epsilon_j < 0$, $\mathrm{Re}\,\epsilon_k < 0$, reads

$$\langle z^{\ddagger}_{\alpha j}(t) z^{\ddagger}_{\alpha k}(0)\rangle_\alpha = \sum_{mn} \kappa_{jm}\kappa_{kn} \int_{-\infty}^{t} d\tau e^{\epsilon_j(t-\tau)} \int_{-\infty}^{0} d\sigma e^{-\epsilon_k \sigma} \times \langle W_{\alpha m}(\tau) W_{\alpha n}(\sigma)\rangle_\alpha. \tag{28}$$

Using Eq. (25), for $t \geqslant 0$ and with

$$K_{jk} = \sum_n \kappa_{jn}\kappa_{kn}, \tag{29}$$

this can be evaluated to

$$\langle z_{\alpha j}^{\ddagger}(t) z_{\alpha k}^{\ddagger}(0)\rangle_{\alpha} = \frac{K_{jk}}{-(\epsilon_j + \epsilon_k)} e^{\epsilon_j t} \quad \text{if Re } \epsilon_j < 0, \quad \text{Re } \epsilon_k < 0. \tag{30a}$$

Similarly,

$$\langle z_{\alpha j}^{\ddagger}(t) z_{\alpha k}^{\ddagger}(0)\rangle_{\alpha} = \frac{K_{jk}}{\epsilon_j + \epsilon_k} e^{\epsilon_k t} \quad \text{if Re } \epsilon_j > 0, \quad \text{Re} \epsilon_k > 0, \tag{30b}$$

$$\langle z_{\alpha j}^{\ddagger}(t) z_{\alpha k}^{\ddagger}(0)\rangle_{\alpha} = \frac{K_{jk}}{\epsilon_j + \epsilon_k} (e^{-\epsilon_k t} - e^{\epsilon_j t}) \quad \text{if Re } \epsilon_j < 0, \quad \text{Re } \epsilon_k > 0, \tag{30c}$$

and

$$\langle z_{\alpha j}^{\ddagger}(t) z_{\alpha k}^{\ddagger}(0)\rangle_{\alpha} = 0 \quad \text{if Re } \epsilon_j > 0, \quad \text{Re } \epsilon_k < 0. \tag{30d}$$

All these correlation functions decay exponentially for long times. Note that that the correlation in Eq. (30d) of an unstable component at a later time $t>0$ with a stable component at time zero vanishes identically because the former depends on the fluctuating force after time t, the latter on the force before time zero. For the same reason, the correlation in Eq. (30c) of a stable component at $t>0$ with an unstable component at time zero vanishes as $t \to 0$.

The correlation functions in Eq. (30) can be evaluated explicitly for one-dimensional dynamics. In this case, the eigenvalues are given by Eq. (15), and the matrix A can be diagonalized by

$$A = M \begin{pmatrix} \epsilon_s & 0 \\ 0 & \epsilon_u \end{pmatrix} M^{-1}, \tag{31}$$

with

$$M = \begin{pmatrix} 1 & 1 \\ \epsilon_s & \epsilon_u \end{pmatrix} \quad \text{and } M^{-1} = \frac{1}{\epsilon_u - \epsilon_s} \begin{pmatrix} \epsilon_u & -1 \\ -\epsilon_s & 1 \end{pmatrix}. \tag{32}$$

In one dimension, the fluctuating force in Eq. (24) can have only one independent component with a scalar coupling strength g, and using Eq. (32) the diagonal coupling strength reduces to

$$\kappa := \kappa_u = -\kappa_s = \frac{g}{\epsilon_u - \epsilon_s}. \tag{33}$$

We will in the following only discuss the correlation functions in Eq. (30) for vanishing time shift $t=0$. The covariances of the stable and unstable components of one-dimensional dynamics reduce to

$$\langle z_u^{\ddagger 2}\rangle_{\alpha} = \frac{\kappa^2}{2\epsilon_u}, \tag{34a}$$

$$\langle z_s^{\ddagger 2}\rangle_{\alpha} = \frac{\kappa^2}{-2\epsilon_s}, \tag{34b}$$

$$\langle z_u^{\ddagger} z_s^{\ddagger}\rangle_{\alpha} = 0. \tag{34c}$$

The variances, Eq. (34), of the stable and unstable components are shown in Fig. 4 as a function of the damping constant γ, which is proportional to the noise strength. Not surprisingly, both variances vanish in the absence of noise ($\gamma=0$). In the limit of strong noise, the variance of the stable component tends to zero as $1/\gamma^2$, whereas the variance of the unstable component approaches its maximum value $k_B T/\omega_b^2$.

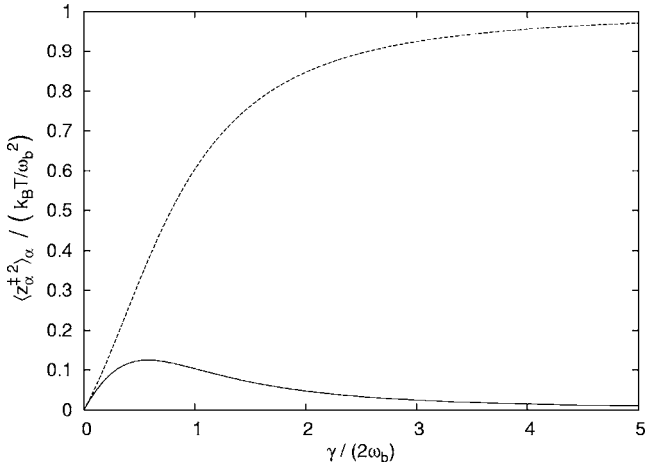

FIG. 4. Variances (34) of stable (solid curve) and unstable (dashed curve) components the TS trajectory $z_{\alpha}^{\ddagger}(t)$ in one dimension.

Using the coordinate transformation in Eq. (32), the diagonal covariances in Eq. (34) can be converted into the covariances of the position $q_{\alpha}^{\ddagger}$ and velocity $v_{\alpha}^{\ddagger}$ of the TS trajectory. They are

$$\langle q_{\alpha}^{\ddagger 2}\rangle_{\alpha} = \Sigma^2, \tag{35a}$$

$$\langle v_{\alpha}^{\ddagger 2}\rangle_{\alpha} = \omega_b^2 \Sigma^2, \tag{35b}$$

$$\langle q_{\alpha}^{\ddagger} v_{\alpha}^{\ddagger}\rangle_{\alpha} = 0, \tag{35c}$$

with

$$\Sigma = \frac{g^2}{2\omega_b^2 \sqrt{\gamma^2 + 4\omega_b^2}}. \tag{36}$$

Somewhat surprisingly, the position and velocity of the TS trajectory turn out to be statistically independent. The variance of the position coordinate is shown in Fig. 5 as a func-

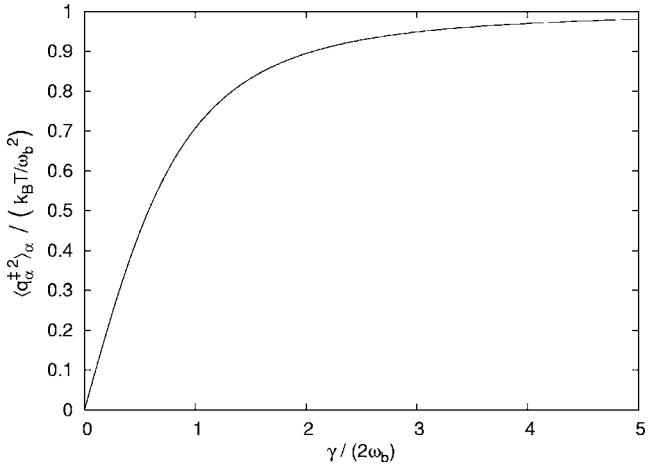

FIG. 5. Variance (36) of the position coordinate of the TS trajectory $z_{\alpha}^{\ddagger}(t)$ in one dimension.

tion of γ. Similar to the behavior of the unstable component, it grows with increasing noise strength from zero to a maximum value of $k_B T/\omega_b^2$.

These geometrical observations lead to a novel interpretation of the friction dependence of reaction rates. In a well-defined reactive system there is a potential well with a stationary population of reactants on one side of the barrier. Only the fraction of the population that lies beyond the stable manifold of the moving reference point, which is very small for small friction, will be reactive. As the friction increases, the reference point moves further down into the reactant well so that a larger portion of the population can at times become reactive. That effect, however, does not grow indefinitely as the friction gets large. Instead, it saturates, so that an opposing effect takes over: As was noted in Sec. IV A, the invariant manifolds of the relative dynamics rotate toward the coordinate axes for large friction, so that the reactive portion of the relative phase space shrinks to zero. This effect eventually leads to turnover and to a decreasing overall reaction rate at very large friction.

D. Stochastic separatrices

The previous construction provides a separation between the dynamics of the barrier crossing, as represented by the relative dynamics, and its statistical properties, which are embodied in the stochastic TS trajectory. The combination of these two aspects allows one to obtain a detailed picture of the barrier crossing. As an example, we present the calculation of the stochastic separatrix near the barrier top, i.e., the collection of all points in phase space for which the reaction probability is 50%.[37]

To this end, pick a point $\mathbf{z}$ in phase space as the initial point, at $t=0$, of a stochastic trajectory. This point can be characterized equivalently either by its coordinates $\mathbf{q}(0)$, $\boldsymbol{v}(0)$ or by the diagonal coordinates $z_s(0)$, $z_u(0)$ in the stable and unstable directions. The latter representation together consist of the unstable degree of freedom—illustrated in Fig. 1(a),—and an arbitrary number of stable transverse coordinates. The fate of a trajectory in the remote future is determined by the relative coordinate $\Delta z_u(0)=z_u(0)-z_{\alpha u}^{\ddagger}(0)$. A trajectory will evolve into products as $t\to\infty$ if $\Delta z_u(0)>0$, i.e., if $z_{\alpha u}^{\ddagger}(0)<z_u(0)$. Because $z_{\alpha u}^{\ddagger}(0)$ is Gaussian distributed with zero mean and a variance σ_u^2 given by (30b) or, in one degree of freedom, by (34a), this probability is easily computed to be

$$P_+ = \frac{1}{2}\,\mathrm{erfc}\left(-\frac{z_u(0)}{\sqrt{2}\sigma_u}\right), \tag{37}$$

in terms of the complementary error function[50]

$$\mathrm{erfc}(x) = \frac{2}{\sqrt{\pi}}\int_x^\infty \exp(-t^2)dt. \tag{38}$$

Similarly, a trajectory will come from the product side in the remote past $t\to-\infty$ if $z_{\alpha s}^{\ddagger}(0)<z_s(0)$, the probability of which is

$$P_- = \frac{1}{2}\,\mathrm{erfc}\left(-\frac{z_s(0)}{\sqrt{2}\sigma_s}\right), \tag{39}$$

with the variance σ_s^2 given by Eq. (30a) or Eq. (30b).

Equations (37) and (39) provide a means to identify the stochastic separatrices, where the probabilities for a trajectory to evolve into reactants or products are both equal to 50%. The stochastic separatrix between trajectories that evolve into reactants or products in the future is the subspace $z_u(0)=0$ according to Eq. (37), whereas the separatrix between reactants and products in the past is $z_s(0)=0$. The present considerations thus reproduce, in a more quantitative way, the result stated in Ref. 37 and at the same time generalize it to systems with arbitrarily many degrees of freedom. Note, however, that the stochastic separatrices separate reactive from nonreactive trajectories only in a probabilistic sense, whereas the moving separatrices introduces in Sec. IV A allow one to determine the fate of a trajectory with certainty.

E. Sampling the TS trajectory

The time correlation functions in Eq. (30) completely specify the probability distribution of the TS trajectory, i.e., the joint distribution of all components of the trajectory at all different times. To use the TS trajectory in numerical work of any kind, it is essential to obtain random samples $\mathbf{z}_\alpha^{\ddagger}(t)$ of the trajectory from this distribution. The obvious way to do so, namely, to generate an instance of the fluctuating force $\boldsymbol{\xi}_\alpha(t)$ and then compute the integrals in Eqs. (20) and (23), would quickly turn out to be prohibitively laborious, so that a more efficient algorithm must be devised.

The problem at hand can be stated more precisely as follows. To sample a representative of the TS trajectory $\mathbf{z}_\alpha^{\ddagger}(t)$ with L equidistant time steps over a time interval $T=L\Delta t$, one has to compute $L+1$ random vectors $\mathbf{z}_\alpha^{\ddagger}(0)$, $\mathbf{z}_\alpha^{\ddagger}(\Delta t),\ldots,\mathbf{z}_\alpha^{\ddagger}(T=L\Delta t)$ from a Gaussian distribution with zero mean and covariances given by Eq. (30). Phrased this way, the problem is to sample a correlated Gaussian random variable with $2N(L+1)$ components. This is easy to do if only a single sample point $\mathbf{z}_\alpha^{\ddagger}(0)$ on the TS trajectory is required, but if the number of sample points is large, it is still a formidable task.

In the case of white noise, this task is greatly simplified by the recurrence relation

$$z_{\alpha j}^{\ddagger}(t+s) = e^{\epsilon_j s}\left(z_{\alpha j}^{\ddagger}(t) + \Delta_{\alpha j}(t,s)\right), \tag{40}$$

where

$$\Delta_{\alpha j}(t,s) = \int_t^{t+s} e^{\epsilon_j(t-\tau)}\xi_j(\tau)d\tau, \tag{41}$$

that can easily be derived from either Eq. (20) or Eq. (23) and holds for both the stable and the unstable components of $\mathbf{z}_\alpha^{\ddagger}(t)$. As the fluctuating force $\xi_{\alpha j}(t)$, the increment functions $\Delta_{\alpha j}(t,s)$ are Gaussian random variables with zero mean. Their covariances can be computed from Eqs. (27) and (25) to be

$$\langle \Delta_{\alpha j}(t,s)\Delta_{\alpha k}(t,s)\rangle_\alpha = \frac{K_{jk}}{\epsilon_j+\epsilon_k}(1-e^{-(\epsilon_j+\epsilon_k)s}), \tag{42}$$

where K_{jk} is given by Eq. (29).

Because for white noise the values of the fluctuating force at different times are independent, the increment functions $\Delta_{\alpha j}(t_1,s_1)$ and $\Delta_{\alpha k}(t_2,s_2)$ are stochastically independent if the time intervals (t_1,t_1+s_1) and (t_2,t_2+s_2) do not overlap, i.e., if $t_1+s_1\leqslant t_2$ or $t_2+s_2\leqslant t_1$. Further, $\Delta_{\alpha j}(t,s)$ is independent of the component $z^{\ddagger}_{\alpha k}(\tau)$ of the TS trajectory whenever either k denotes a stable direction with Re $\epsilon_k<0$ and $\tau\leqslant t$ or k denotes an unstable direction with Re $\epsilon_k>0$ and $\tau\geqslant t+s$.

These observations lead to the following algorithm for sampling the TS trajectory. Generate random values for the stable components $z^{\ddagger}_{\alpha j}(0)$ at time zero using the correlation function, Eq. (30a). Generate values for the unstable component $z^{\ddagger}_{\alpha j}(T)$ at time T. They are independent of the stable components computed before. Typically, there will be only one stable component. Generate increment vectors $\mathbf{\Delta}_\alpha(l\Delta t,\Delta t)$ for $l=0,1,\ldots,L-1$ using the covariances, Eq. (42). Increments for different l are independent. Using these increments and the recurrence relation in Eq. (40), compute the stable components $z_{\alpha j}(l\Delta t)$ for $l=1,2,\ldots,L$. This recursion is numerically stable because the exponential factor in Eq. (40) has an absolute value less than 1. The unstable components $z_{\alpha j}(l\Delta t)$ are computed using the same recurrence relation, Eq. (40), in the opposite order, starting from $l=L-1,\ldots,0$. Again, the recursion is numerically stable. This algorithm allows one to sample an arbitrary stretch of the TS trajectory without ever having to compute correlated random variables of a dimension larger than the phase-space dimension $2N$.

V. THE TRANSITION STATE IN COLORED NOISE

It might seem at first sight that in the derivation of the TS trajectory in Sec. IV B we have never used the assumption that the fluctuating force $\boldsymbol{\xi}_\alpha(t)$ represents white noise and that, therefore, the results in Eqs. (20) and (23) for $\mathbf{z}^{\ddagger}_\alpha(t)$ are equally valid if the noise is colored. However, if the values of the fluctuating force $\xi_\alpha(t)$ at different times are statistically correlated, the fluctuation-dissipation theorem demands the occurrence of memory friction effects, and the Langevin equation, Eq. (3), must be replaced with the generalized Langevin equation[38,39,41–45,51]

$$\ddot{\mathbf{q}}_\alpha(t)=\mathbf{\Omega}\mathbf{q}_\alpha(t)-\int_{-\infty}^{t}d\tau\mathbf{\Gamma}(t-\tau)\dot{\mathbf{q}}_\alpha(\tau)+\boldsymbol{\xi}_\alpha(t), \tag{43}$$

where the symmetric-matrix valued function $\mathbf{\Gamma}(t)$ is related to the fluctuating force by

$$\langle \boldsymbol{\xi}_\alpha(t)\boldsymbol{\xi}^T_\alpha(s)\rangle_\alpha = k_{\mathrm{B}}T\mathbf{\Gamma}(|t-s|). \tag{44}$$

With the definition

$$\mathbf{\Gamma}(t)=0 \quad \text{if } t<0, \tag{45}$$

the upper limit of integration in Eq. (43) can be extended to infinity.

Because the friction force in Eq. (43) depends on the entire prehistory of the trajectory rather than only the present velocity, Eq. (43) cannot be solved as an initial value problem. Instead, the entire trajectory up to the present time must be specified before its further evolution can be determined. Although this freedom seems to render the phase space of Eq. (43) infinite dimensional, we will show below that in many cases the phase-space dimension is actually finite because only those initial trajectories can be prescribed that themselves satisfy Eq. (43).

To solve the GLE, Eq. (43), we use the bilateral Laplace transform,

$$\hat{\mathbf{q}}(\epsilon)=\int_{-\infty}^{\infty}dte^{-\epsilon t}\mathbf{q}(t), \tag{46}$$

and its inverse,[52]

$$\mathbf{q}(t)=\frac{1}{2\pi i}\int_{-i\infty}^{i\infty}d\epsilon e^{\epsilon t}\hat{\mathbf{q}}(\epsilon). \tag{47}$$

It transforms Eq. (43) into

$$(\epsilon^2+\epsilon\hat{\mathbf{\Gamma}}(\epsilon)-\mathbf{\Omega})\hat{\mathbf{q}}_\alpha(\epsilon)=\hat{\boldsymbol{\xi}}_\alpha(\epsilon). \tag{48}$$

Using Eq. (45), the bilateral Laplace transform $\hat{\mathbf{\Gamma}}$ of the friction kernel coincides with the customary one-sided Laplace transform and is holomorphic on a right half plane of the complex ϵ plane that, for bounded $\mathbf{\Gamma}(t)$, includes the half plane Re $\epsilon>0$. We further assume $\hat{\mathbf{\Gamma}}(\epsilon)$ to be meromorphic on the entire complex plane.

A. Relative dynamics

The relative coordinate $\Delta\mathbf{q}(t)$, which is again given by Eq. (6), satisfies the noiseless version of Eq. (48), viz.,

$$(\epsilon^2+\epsilon\hat{\mathbf{\Gamma}}(\epsilon)-\mathbf{\Omega})\Delta\hat{\mathbf{q}}(\epsilon)=0. \tag{49}$$

The general solution of Eq. (49) reads

$$\Delta\hat{\mathbf{q}}(\epsilon)=\sum_j c_j\boldsymbol{\nu}_j\delta(\epsilon-\epsilon_j), \tag{50}$$

corresponding to

$$\Delta\mathbf{q}(t)=\sum_j c_j\boldsymbol{\nu}_j e^{\epsilon_j t}, \tag{51}$$

where c_j are arbitrary constants and ϵ_j, $\boldsymbol{\nu}_j$ denote a complete linear independent set of solutions of the nonlinear eigenvalue equation

$$(\epsilon_j^2+\epsilon_j\hat{\mathbf{\Gamma}}(\epsilon_j)-\mathbf{\Omega})\boldsymbol{\nu}_j=0, \quad \boldsymbol{\nu}_j^2=1. \tag{52}$$

Because the friction kernel $\mathbf{\Gamma}(t)$ is real, its Laplace transform satisfies $\hat{\mathbf{\Gamma}}(\epsilon^*)=\hat{\mathbf{\Gamma}}(\epsilon)^*$, where the asterisk denotes complex conjugation, so that the eigenvalues and eigenvectors of Eq. (52) are either real or occur in complex conjugate pairs. In the latter case, the constants c_j must also be chosen in conjugate pairs to make $\Delta\mathbf{q}(t)$ real. The solution, Eq. (51), of the relative dynamics is exactly analogous to the solution, Eq. (14), in the case of white noise, except that the eigenvalues and eigenvectors are computed differently. The construction of invariant manifolds and a no-recrossing surface that we have given in Sec. IV A therefore carries over unchanged to

colored noise. A trajectory is specified by prescribing the constants c_j. In other words, the dimension of the phase space of the generalized Langevin equation, Eq. (43), is the number of solutions of the nonlinear eigenvalue Eq. (52). That number is typically larger than the phase-space dimension $2N$ of the memoryless Langevin equation, Eq. (3), but still finite if the friction kernel decays exponentially. The phase space is described implicitly by Eq. (51).

B. The transition-state trajectory

A particular solution of Eq. (48) in the presence of the fluctuating force can be found by solving for $\hat{\mathbf{q}}(\epsilon)$ using the inverse Laplace transform (47),

$$\mathbf{q}_\alpha^\ddagger(t) = \frac{1}{2\pi i}\int_{-i\infty}^{i\infty} d\epsilon e^{\epsilon t}(\epsilon^2 + \epsilon\hat{\mathbf{\Gamma}}(\epsilon) - \mathbf{\Omega})^{-1}\hat{\boldsymbol{\xi}}_\alpha(\epsilon). \tag{53}$$

With the definition of $\hat{\boldsymbol{\xi}}(\epsilon)$ and after the order of integration is interchanged, Eq. (53) takes the form

$$\mathbf{q}_\alpha^\ddagger(t) = \int_{-\infty}^{\infty} d\tau\left[\frac{1}{2\pi i}\int_{-i\infty}^{i\infty} d\epsilon e^{\epsilon(t-\tau)}(\epsilon^2 + \epsilon\hat{\mathbf{\Gamma}}(\epsilon) - \mathbf{\Omega})^{-1}\right]\boldsymbol{\xi}_\alpha(\tau). \tag{54}$$

The integral over ϵ can be evaluated using the calculus of residues if the contour of integration is closed through the left half plane if $\tau<t$ and through the right half plane if $\tau>t$. The poles of the integrand are precisely the eigenvalues ϵ_j, where the matrix of Eq. (52) is not invertible. The residue of the matrix inverse in (54) at $\epsilon=\epsilon_j$ is denoted by $\boldsymbol{\mu}_j$, so that

$$\mathbf{q}_\alpha^\ddagger(t) = \sum_j \mathbf{q}_{\alpha j}^\ddagger(t), \tag{55}$$

with

$$\mathbf{q}_{\alpha j}^\ddagger(t) = \boldsymbol{\mu}_j\int_{-\infty}^{t} d\tau e^{\epsilon_j(t-\tau)}\boldsymbol{\xi}_\alpha(\tau) = \boldsymbol{\mu}_j\int_{-\infty}^{0} d\tau e^{-\epsilon_j\tau}\boldsymbol{\xi}_\alpha(t+\tau), \tag{56}$$

if Re $\epsilon_j<0$ and

$$\mathbf{q}_{\alpha j}^\ddagger(t) = -\boldsymbol{\mu}_j\int_{t}^{\infty} d\tau e^{\epsilon_j(t-\tau)}\boldsymbol{\xi}_\alpha(\tau) = -\boldsymbol{\mu}_j\int_{0}^{\infty} d\tau e^{-\epsilon_j\tau}\boldsymbol{\xi}_\alpha(t+\tau), \tag{57}$$

if Re $\epsilon_j>0$. These solutions are close analogs of Eqs. (20) and (23) in the case of white noise, with the residue factors $\boldsymbol{\mu}_j$ replacing the projection onto the eigenspace j. The components $q_{\alpha j}^\ddagger$ can easily be verified to satisfy the equation of motion

$$\dot{\mathbf{q}}_{\alpha j}^\ddagger(t) = \epsilon_j\mathbf{q}_{\alpha j}^\ddagger(t) + \boldsymbol{\mu}_j\boldsymbol{\xi}_\alpha(t) \tag{58}$$

that is expected for a component in an eigenspace of the noiseless dynamics with eigenvalue ϵ_j. Again, the residues $\boldsymbol{\mu}_j$ play the role of the projection onto the eigenspace j.

A more explicit form of the residues $\boldsymbol{\mu}_j$ can be found as follows: First, by observing that

$$\boldsymbol{A}(\epsilon) = \epsilon^2 + \epsilon\hat{\mathbf{\Gamma}}(\epsilon) - \mathbf{\Omega} \tag{59}$$

is a symmetric matrix, we immediately conclude that $\boldsymbol{\mu}_j(=\boldsymbol{\mu}_j^T)$ is also symmetric. For any fixed ϵ, the matrix $\boldsymbol{A}(\epsilon)$ possesses a complete set of eigenvalues $\eta_i(\epsilon)$ and orthonormal eigenvectors $\mathbf{w}_i(\epsilon)$,

$$\begin{aligned}&\boldsymbol{A}(\epsilon)\mathbf{w}_i(\epsilon) = \eta_i(\epsilon)\mathbf{w}_i(\epsilon),\\ &\mathbf{w}_i(\epsilon)\cdot\mathbf{w}_j(\epsilon) = \delta_{ij}.\end{aligned} \tag{60}$$

In terms of its eigensystem, the matrix $\boldsymbol{A}(\epsilon)$ can be written as

$$\boldsymbol{A}(\epsilon) = \sum_i \eta_i(\epsilon)\mathbf{w}_i(\epsilon)\mathbf{w}_i^T(\epsilon), \tag{61}$$

so that

$$\boldsymbol{A}^{-1}(\epsilon) = \sum_i \frac{1}{\eta_i(\epsilon)}\mathbf{w}_i(\epsilon)\mathbf{w}_i^T(\epsilon). \tag{62}$$

When ϵ is equal to a solution ϵ_j of the nonlinear eigenvalue problem in Eq. (52), one of the eigenvalues η_i vanishes, say, $\eta_1(\epsilon_j)=0$, and $\mathbf{w}_1(\epsilon_j)=\boldsymbol{v}_j$. If all the eigenvalues are simple, only the term $i=1$ in Eq. (62) has a pole at $\epsilon=\epsilon_j$, and its residue is

$$\boldsymbol{\mu}_j = \kappa_j\boldsymbol{v}_j\boldsymbol{v}_j^T, \tag{63}$$

where

$$\kappa_j = \frac{1}{\eta_1'(\epsilon_j)}, \tag{64}$$

and the prime denotes the derivative with respect to ϵ. The residue $\boldsymbol{\mu}_j$ is thus proportional to the geometric projection onto the eigenvector $\boldsymbol{v}_j$, with the factor κ_j describing the strength of the coupling of the noise to the particular eigenmode. Using first-order perturbation theory, this factor is found to be

$$\kappa_j = \frac{1}{2\epsilon_j + \boldsymbol{v}_j^T(\hat{\mathbf{\Gamma}}(\epsilon_j) + \epsilon_j\hat{\mathbf{\Gamma}}'(\epsilon_j))\boldsymbol{v}_j}. \tag{65}$$

The representation, Eq. (63), of the residues leads to a more explicit form of the components $q_{\alpha j}^\ddagger(t)$,

$$\mathbf{q}_{\alpha j}^\ddagger(t) = \kappa_j\boldsymbol{v}_j\int_{-\infty}^{0} d\tau e^{-\epsilon_j\tau}\boldsymbol{v}_j\cdot\boldsymbol{\xi}_\alpha(t+\tau), \tag{66}$$

if Re $\epsilon_j<0$, and a similar expression for Re $\epsilon_j>0$. Note that $\mathbf{q}_{\alpha j}^\ddagger(t)$ is a scalar multiple of the eigenvector $\boldsymbol{v}_j$.

The eigenvectors of the linear eigenvalue problem in Eq. (60) satisfy the completeness condition

$$\sum_i \mathbf{w}_i\mathbf{w}_i^T = \boldsymbol{I}, \tag{67}$$

where $\boldsymbol{I}$ is the $N\times N$ unit matrix. Because the eigenvalue problem in Eq. (52) is nonlinear, the analogous relation for the $\boldsymbol{v}_j$ does not hold. Instead, if $\hat{\mathbf{\Gamma}}(\epsilon)$ is meromorphic at infinity, the residues $\boldsymbol{\mu}_j$ satisfy the completeness conditions

$$\sum_j \boldsymbol{\mu}_j = \sum_j \kappa_j\boldsymbol{v}_j\boldsymbol{v}_j'^T = 0, \tag{68a}$$

$$\sum_j \epsilon_j \boldsymbol{\mu}_j = \sum_j \kappa_j \epsilon_j \boldsymbol{v}_j \boldsymbol{v}_j'^T = \boldsymbol{I}. \tag{68b}$$

To see this, note that

$$\sum_j \boldsymbol{\mu}_j = \frac{1}{2\pi i} \oint_{\mathcal{C}} d\epsilon (\epsilon^2 + \epsilon \hat{\boldsymbol{\Gamma}}(\epsilon) - \boldsymbol{\Omega})^{-1}, \tag{69}$$

where $\mathcal{C}$ is a contour in the complex ϵ plane that encircles all eigenvalues ϵ_j in the clockwise direction. With $\theta = 1/\epsilon$, Eq. (69) reads

$$\sum_j \boldsymbol{\mu}_j = \frac{1}{2\pi i} \oint_{1/\mathcal{C}} d\theta (\boldsymbol{I} + \theta \hat{\boldsymbol{\Gamma}}(1/\theta) - \theta^2 \boldsymbol{\Omega})^{-1}, \tag{70}$$

where the contour $1/\mathcal{C}$ is again oriented clockwise. By construction, it encircles none of the inverse eigenvalues $1/\epsilon_j$. As the integrand is furthermore regular at $\theta = 0$, the integral is zero, thus proving Eq. (68a). To prove Eq. (68b), a similar computation leads to

$$\begin{aligned} \sum_j \epsilon_j \boldsymbol{\mu}_j &= \frac{1}{2\pi i} \oint_{\mathcal{C}} d\epsilon \epsilon (\epsilon^2 + \epsilon \hat{\boldsymbol{\Gamma}}(\epsilon) - \boldsymbol{\Omega})^{-1} \\ &= \frac{1}{2\pi i} \oint_{1/\mathcal{C}} \frac{d\theta}{\theta} (\boldsymbol{I} + \theta \hat{\boldsymbol{\Gamma}}(1/\theta) - \theta^2 \boldsymbol{\Omega})^{-1} = \boldsymbol{I}, \end{aligned} \tag{71}$$

where the last equality holds because the integrand in Eq. (71) has a simple pole at $\theta = 0$.

C. Statistical properties of the TS trajectory

As in the case of white noise, the components of the TS trajectory, Eqs. (56) and (57), are Gaussian distributed with zero mean if the noise $\boldsymbol{\xi}_\alpha(t)$ is. To specify their distribution completely, it remains only to compute their time correlation functions. For $t > 0$ and in the case of two stable components with Re $\epsilon_j < 0$, Re $\epsilon_k < 0$, they are

$$\begin{aligned} \langle \mathbf{q}_{\alpha j}^{\ddagger}(t) \mathbf{q}_{\alpha k}^{\ddagger T}(0) \rangle_\alpha &= \boldsymbol{\mu}_j \int_{-\infty}^{t} d\tau \int_{-\infty}^{0} d\sigma e^{-\epsilon_j(\tau - t)} e^{-\epsilon_k \sigma} \\ &\quad \times \langle \boldsymbol{\xi}_\alpha(\tau) \boldsymbol{\xi}_\alpha(\sigma) \rangle_\alpha \boldsymbol{\mu}_k^T = k_B T \boldsymbol{\mu}_j \boldsymbol{I}_{jk}(t) \boldsymbol{\mu}_k, \end{aligned} \tag{72}$$

with the matrix-valued correlation integral

$$\boldsymbol{I}_{jk}(t) = \int_{-\infty}^{t} d\tau \int_{-\infty}^{0} d\sigma e^{\epsilon_j(t-\tau)} e^{-\epsilon_k \sigma} \boldsymbol{\Gamma}(|\tau - \sigma|). \tag{73}$$

Recall that $\boldsymbol{\mu}_k$ is symmetric, and note that the time-correlation matrix in Eq. (72) is a scalar multiple of the matrix $\boldsymbol{v}_j \boldsymbol{v}_k^T$ if Eq. (63) holds.

To evaluate the correlation integral in Eq. (73), we split the range of the τ integration into the intervals $(-\infty, 0)$ and $(0, t)$. The latter part can then be expressed through the function

$$\boldsymbol{C}(\zeta_1, \zeta_2, t) = \int_0^t d\tau \int_0^\infty d\sigma e^{\zeta_1(t-\tau)} e^{-\zeta_2 \sigma} \boldsymbol{\Gamma}(\tau + \sigma). \tag{74}$$

The former part, apart from a factor $e^{\epsilon_j t}$, is

$$\boldsymbol{I}_{jk}(0) = \int_{-\infty}^{0} d\tau \int_{-\infty}^{0} d\sigma e^{-\epsilon_j \tau} e^{-\epsilon_k \sigma} \boldsymbol{\Gamma}(|\tau - \sigma|), \tag{75}$$

which in terms of $\chi = \tau - \sigma$ and $\psi = \tau + \sigma$, can be rewritten as

$$\begin{aligned} \boldsymbol{I}_{jk}(0) &= \frac{1}{2} \int_{-\infty}^{\infty} d\chi \boldsymbol{\Gamma}(|\chi|) e^{(\epsilon_k - \epsilon_j)\chi/2} \int_{-\infty}^{|\chi|} d\psi e^{-(\epsilon_j + \epsilon_k)\psi/2} \\ &= \frac{1}{-(\epsilon_j + \epsilon_k)} \left(\int_{-\infty}^{0} d\chi e^{\epsilon_k \chi} \boldsymbol{\Gamma}(-\chi) + \int_0^\infty d\chi e^{-\epsilon_j \chi} \boldsymbol{\Gamma}(\chi) \right) \\ &= \frac{1}{-(\epsilon_j + \epsilon_k)} (\hat{\boldsymbol{\Gamma}}(-\epsilon_j) + \hat{\boldsymbol{\Gamma}}(-\epsilon_k)). \end{aligned} \tag{76}$$

The correlation integral in Eq. (73) thus finally reads

$$\boldsymbol{I}_{jk}(t) = \frac{e^{\epsilon_j t}}{-(\epsilon_j + \epsilon_k)} (\hat{\boldsymbol{\Gamma}}(-\epsilon_j) + \hat{\boldsymbol{\Gamma}}(-\epsilon_k)) + \boldsymbol{C}(\epsilon_j, -\epsilon_k, t),$$

$$\text{if Re } \epsilon_j < 0, \quad \text{Re } \epsilon_k < 0. \tag{77a}$$

The correlation functions involving unstable components take the same general form of Eq. (72) with

$$\boldsymbol{I}_{jk}(t) = \frac{e^{-\epsilon_k t}}{\epsilon_j + \epsilon_k} (\hat{\boldsymbol{\Gamma}}(\epsilon_j) + \hat{\boldsymbol{\Gamma}}(\epsilon_k)) + \boldsymbol{C}(-\epsilon_k, \epsilon_j, t)$$

$$\text{if Re } \epsilon_j > 0, \quad \text{Re } \epsilon_k > 0, \tag{77b}$$

$$\boldsymbol{I}_{jk}(t) = \frac{e^{-\epsilon_k t}}{\epsilon_j + \epsilon_k} (\hat{\boldsymbol{\Gamma}}(\epsilon_k) + \hat{\boldsymbol{\Gamma}}(-\epsilon_k)) - \frac{e^{\epsilon_j t}}{\epsilon_j + \epsilon_k} (\hat{\boldsymbol{\Gamma}}(-\epsilon_j) + \hat{\boldsymbol{\Gamma}}(-\epsilon_k)) + \boldsymbol{C}(\epsilon_j, -\epsilon_k, t) \quad \text{if Re } \epsilon_j < 0, \quad \text{Re } \epsilon_k > 0, \tag{77c}$$

$$\boldsymbol{I}_{jk}(t) = \frac{e^{\epsilon_j t}}{\epsilon_j + \epsilon_k} (\hat{\boldsymbol{\Gamma}}(\epsilon_j) - \hat{\boldsymbol{\Gamma}}(-\epsilon_k)) + \boldsymbol{C}(\epsilon_j, -\epsilon_k, t)$$

$$\text{if Re } \epsilon_j > 0, \quad \text{Re } \epsilon_k < 0. \tag{77d}$$

All correlation integrals consist of exponentially decaying contributions and a correction term $\boldsymbol{C}$. The latter can be written as

$$\boldsymbol{C}(\zeta_1, \zeta_2, t) = \int_0^t d\tau e^{\zeta_1(t-\tau)} \hat{\boldsymbol{\Gamma}}_\tau(\zeta_2), \tag{78}$$

where $\hat{\boldsymbol{\Gamma}}_\tau$ denotes the Laplace transform of the time-shifted function $\boldsymbol{\Gamma}(t + \tau)$. Unless $\hat{\boldsymbol{\Gamma}}(\epsilon)$ is growing at least exponentially as $|\epsilon| \to \infty$ and Re $\epsilon < 0$, an explicit expression for the correction term $\boldsymbol{C}$ can be found. To this end, use the definition of $\hat{\boldsymbol{\Gamma}}_\tau$ and the inverse Laplace transform, Eq. (47), to write, for Re $\epsilon > 0$,

$$\begin{aligned} \hat{\boldsymbol{\Gamma}}_\tau(\epsilon) &= \int_0^\infty d\sigma e^{-\epsilon\sigma} \frac{1}{2\pi i} \int_{-i\infty}^{i\infty} d\eta e^{\eta(\sigma + \tau)} \hat{\boldsymbol{\Gamma}}(\eta) \\ &= \frac{1}{2\pi i} \int_{-i\infty}^{i\infty} d\eta e^{\eta\tau} \frac{\hat{\boldsymbol{\Gamma}}(\eta)}{\epsilon - \eta}. \end{aligned} \tag{79}$$

If it is now permissible to close the integration contour through the left half plane, Eq. (79) yields

$$\hat{\mathbf{\Gamma}}_\tau(\epsilon) = \sum_i \frac{\nu_i}{\epsilon - E_i} e^{E_i \tau}, \tag{80}$$

where E_i are the poles of $\hat{\mathbf{\Gamma}}(\epsilon)$ in the left half plane (which typically are all poles) and ν_i are the corresponding residues. The correction term $\boldsymbol{C}$ thus reads

$$\boldsymbol{C}(\zeta_1, \zeta_2, t) = \sum_i \frac{\nu_i}{(E_i - \zeta_1)(E_i - \zeta_2)} (e^{\zeta_1 t} - e^{E_i t}) \tag{81}$$

and is also exponentially decaying.

D. Reconstructing the eigenvalues

The dynamics of the GLE, Eq. (43), is characterized by the eigenvalues ϵ_j. If the TS trajectory does indeed capture the essential aspects of the dynamics, it should enable us to identify the eigenvalues. In particular, we should be able to find the Grote-Hynes reaction frequency,[32,51] viz., the unique eigenvalue with positive real part, that approximately describes the influence of colored noise on the reaction rate. That this information can actually be obtained from the TS trajectory can be seen most easily by examining the statistical properties of its Laplace transform rather than the time-correlation functions of the TS trajectory directly. According to Eq. (53),

$$\hat{\mathbf{q}}_\alpha^\ddagger(\epsilon) = (\epsilon^2 + \epsilon \hat{\mathbf{\Gamma}}(\epsilon) - \mathbf{\Omega})^{-1} \hat{\boldsymbol{\xi}}_\alpha(\epsilon). \tag{82}$$

This Laplace transform has poles at the eigenvalues ϵ_j. In addition, there are the random poles of the Laplace transform $\hat{\boldsymbol{\xi}}_\alpha(\epsilon)$ of the noise. Thus, the eigenvalues of the noiseless dynamics cannot be determined from the Laplace transform of a single instance of the TS trajectory. If, however, the Laplace transform of several instances of $\mathbf{q}_\alpha^\ddagger$ is given, the eigenvalues can be discerned with certainty because they are fixed whereas the poles of $\hat{\boldsymbol{\xi}}_\alpha(\epsilon)$ are random.

The randomness of the poles is entirely absent from the correlation function of $\hat{\mathbf{q}}_\alpha^\ddagger$, which is

$$\langle \hat{\mathbf{q}}_\alpha^\ddagger(\epsilon) \hat{\mathbf{q}}_\alpha^{\ddagger T}(\epsilon') \rangle_\alpha = (\epsilon^2 + \epsilon \hat{\mathbf{\Gamma}}(\epsilon) - \mathbf{\Omega})^{-1} \langle \hat{\boldsymbol{\xi}}_\alpha(\epsilon) \hat{\boldsymbol{\xi}}_\alpha^T(\epsilon') \rangle_\alpha \times (\epsilon'^2 + \epsilon' \hat{\mathbf{\Gamma}}(\epsilon') - \mathbf{\Omega})^{-1}. \tag{83}$$

If the Laplace transform $\hat{\boldsymbol{\xi}}_\alpha(\epsilon)$ is replaced with its definition in Eq. (46), the remaining average turns out to be

$$\langle \hat{\boldsymbol{\xi}}_\alpha(\epsilon) \hat{\boldsymbol{\xi}}_\alpha^T(\epsilon') \rangle_\alpha = \int_0^\infty d\tau \int_0^\infty d\sigma e^{-\epsilon \tau} e^{-\epsilon' \sigma} \mathbf{\Gamma}(|\tau - \sigma|). \tag{84}$$

In the notation of Sec. V C, Eq. (84) is the correlation integral $\boldsymbol{I}_{\epsilon\epsilon'}(0)$ between two unstable components. It has already been evaluated in Eq. (77b) to be

$$\langle \hat{\boldsymbol{\xi}}_\alpha(\epsilon) \hat{\boldsymbol{\xi}}_\alpha^T(\epsilon') \rangle_\alpha = \frac{\hat{\mathbf{\Gamma}}(\epsilon) + \hat{\mathbf{\Gamma}}(\epsilon')}{\epsilon + \epsilon'}. \tag{85}$$

Therefore,

$$\langle \hat{\mathbf{q}}_\alpha^\ddagger(\epsilon) \hat{\mathbf{q}}_\alpha^{\ddagger T}(\epsilon') \rangle_\alpha = (\epsilon^2 + \epsilon \hat{\mathbf{\Gamma}}(\epsilon) - \mathbf{\Omega})^{-1} \frac{\hat{\mathbf{\Gamma}}(\epsilon) + \hat{\mathbf{\Gamma}}(\epsilon')}{\epsilon + \epsilon'} \times (\epsilon'^2 + \epsilon' \hat{\mathbf{\Gamma}}(\epsilon') - \mathbf{\Omega})^{-1}, \tag{86}$$

and, in particular, for $\epsilon = \epsilon'$,

$$\langle \hat{\mathbf{q}}_\alpha^\ddagger(\epsilon) \hat{\mathbf{q}}_\alpha^{\ddagger T}(\epsilon) \rangle_\alpha = (\epsilon^2 + \epsilon \hat{\mathbf{\Gamma}}(\epsilon) - \mathbf{\Omega})^{-1} \frac{\hat{\mathbf{\Gamma}}(\epsilon)}{\epsilon} (\epsilon^2 + \epsilon \hat{\mathbf{\Gamma}}(\epsilon) - \mathbf{\Omega})^{-1}. \tag{87}$$

This correlation function has poles at $\epsilon = 0$, at the poles of $\hat{\mathbf{\Gamma}}(\epsilon)$ and at the eigenvalues of the noiseless dynamics. Usually, the friction kernel $\mathbf{\Gamma}$ will be known, so that the eigenvalues ϵ_j can be determined from Eq. (87). On the other hand, even if the friction kernel is unknown, the eigenvalues can be discerned because they are double poles of Eq. (87), whereas the poles of $\hat{\mathbf{\Gamma}}(\epsilon)$ will typically be simple. In particular, the Grote-Hynes frequency[32,51] can be identified as the only pole of the correlation function in Eq. (87) that has a positive real part.

VI. CONCLUSIONS AND OUTLOOK

To generalize the formalism of TST to reactive systems driven by noise, we have introduced a time-dependent dividing surface that is stochastically moving in phase space so that it is crossed once and only once by each transition path. This construction requires the identification of a privileged stochastic trajectory that remains in the vicinity of the barrier for all times. This TS trajectory serves as the origin of a stochastically moving coordinate system that carries the no-recrossing TS dividing surface for the noiseless dynamics. The moving no-recrossing dividing surface thus obtained describes a reaction in the same way as a static dividing surface in conventional TST and therefore provides a novel approach to the theory of reaction dynamics in a noisy environment. The challenge lying ahead is to determine a rate formula that makes optimal use of the geometric objects associated with the TS trajectory and the moving no-recrossing TS dividing surface.

The further generalization of this approach to all-atom representations of solvated chemical reactions is nontrivial. In the Langevin models, the noise sequence can be specified independently of the reaction path or the solvent modes. For an all-atom solvent, by contrast, this is impossible because the noise sequence depends on the trajectory of the chosen coordinates identifying the reaction. A given solvation-shell structure creates an effective cavity that accomodates a particular set of reaction geometries more easily than others. Thus a critical question to be pursued in future work is how to identify the reaction geometry of the moving TS dividing surface in all-atom representations of a solvated chemical reaction.

ACKNOWLEDGMENTS

This work was partly supported by the US National Science Foundation and by the Alexander von Humboldt-Foundation.

[1] W. H. Miller, Faraday Discuss. Chem. Soc. **110**, 1 (1998).
[2] D. G. Truhlar, B. C. Garrett, and S. J. Klippenstein, J. Phys. Chem. **100**, 12771 (1996).
[3] C. Jaffé, S. Kawai, J. Palacián, P. Yanguas, and T. Uzer, Adv. Chem. Phys. **130A**, 171 (2005).
[4] E. P. Wigner, J. Chem. Phys. **7**, 646 (1939).
[5] E. P. Wigner, Trans. Faraday Soc. **34**, 29 (1938).
[6] H. Eyring, J. Chem. Phys. **3**, 107 (1935).
[7] J. C. Keck, Adv. Chem. Phys. **13**, 85 (1967).
[8] M. L. Goldberger and K. M. Watson, *Collision Theory* (Wiley, New York, 1964).
[9] Theory of Chemical Reaction Dynamics, edited by M. Baer (CRC, Boca Raton, FL, 1985), Vols. 1–4.
[10] W. H. Miller, Acc. Chem. Res. **26**, 174 (1993).
[11] P. Pechukas and F. J. Lafferty, J. Chem. Phys. **58**, 1622 (1973).
[12] D. G. Truhlar and B. C. Garrett, Annu. Rev. Phys. Chem. **35**, 159 (1984).
[13] E. Pollak, in *Theory of Chemical Reaction Dynamics*, edited by M. Baer (CRC, Boca Raton, FL, 1985), Vol. 3.
[14] P. Pechukas and E. Pollak, J. Chem. Phys. **71**, 2062 (1979).
[15] T. Komatsuzaki and R. S. Berry, J. Chem. Phys. **110**, 9160 (1999).
[16] S. Wiggins, L. Wiesenfeld, C. Jaffé, and T. Uzer, Phys. Rev. Lett. **86**, 5478 (2001).
[17] T. Uzer, C. Jaffé, J. Palacian, P. Yanguas, and S. Wiggins, Nonlinearity **15**, 957 (2002).
[18] J. T. Hynes, Annu. Rev. Phys. Chem. **36**, 573 (1985).
[19] E. Pollak and P. Talkner, Chaos **15**, 026116 (2005).
[20] B. J. Berne, M. Borkovec, and J. E. Straub, J. Phys. Chem. **92**, 3711 (1988).
[21] E. Pollak, in *Dynamics of Molecules and Chemical Reactions*, edited by R. E. Wyatt and J. Zhang (Marcel Dekker, New York, 1996), pp. 617–669.
[22] E. Pollak, J. Chem. Phys. **93**, 1116 (1990).
[23] E. Pollak, J. Chem. Phys. **96**, 8877 (1992).
[24] S. C. Tucker and E. Pollak, J. Stat. Phys. **66**, 975 (1992).
[25] S. C. Tucker, in *New Trends in Kramers' Reaction Rate Theory*, edited by P. Hänggi and P. Talkner (Kluwer, The Netherlands, 1995), pp. 5–46.
[26] C. Dellago, P. Bolhuis, F. S. Csajka, and D. Chandler, J. Chem. Phys. **108**, 1964 (1998).
[27] C. P. Dellago, P. Bolhuis, and D. Chandler, J. Chem. Phys. **110**, 6617 (1999).
[28] P. G. Bolhuis, C. P. Dellago, and D. Chandler, Proc. Natl. Acad. Sci. U.S.A. **97**, 5877 (2000).
[29] P. G. Bolhuis, D. Chandler, C. Dellago, and P. Geissler, Annu. Rev. Phys. Chem. **53**, 291 (2002).
[30] C. Dellago, P. G. Bolhuis, and P. Geissler, Adv. Chem. Phys. **123**, 1 (2002).
[31] T. Bartsch, R. Hernandez, and T. Uzer, Phys. Rev. Lett. **95**, 058301 (2005).
[32] E. Pollak, J. Chem. Phys. **85**, 865 (1986).
[33] R. Zwanzig, J. Stat. Phys. **9**, 215 (1973).
[34] A. O. Caldeira and A. J. Leggett, Phys. Rev. Lett. **46**, 211 (1981); Ann. Phys. (N.Y.) **149**, 374 (1983).
[35] E. Pollak, H. Grabert, and P. Hänggi, J. Chem. Phys. **91**, 4073 (1989).
[36] R. Graham, J. Stat. Phys. **60**, 675 (1990).
[37] C. C. Martens, J. Chem. Phys. **116**, 2516 (2002).
[38] R. Zwanzig, *Nonequilibrium Statistical Mechanics* (Oxford University Press, London, 2001).
[39] P. Hänggi, P. Talkner, and M. Borkovec, Rev. Mod. Phys. **62**, 251 (1990), and references therein.
[40] H. A. Kramers, Physica (Utrecht) **7**, 284 (1940).
[41] R. Zwanzig, Phys. Rev. **124**, 983 (1961).
[42] R. Zwanzig, in *Lectures in Theoretical Physics (Boulder)*, edited by W. E. Brittin, B. W. Downs, and J. Downs (Wiley-Interscience, New York, 1961), Vol. 3, pp. 106–141.
[43] J. Prigogine and P. Resibois, Physica (Amsterdam) **27**, 629 (1961).
[44] H. Mori, Prog. Theor. Phys. **33**, 423 (1965).
[45] R. F. Fox, Phys. Rep. **48**, 180 (1978).
[46] C. Jaffé, D. Farrelly, and T. Uzer, Phys. Rev. Lett. **84**, 610 (2000); Phys. Rev. A **60**, 3833 (1999).
[47] G. W. Ford, M. Kac, and P. Mazur, J. Math. Phys. **6**, 504 (1965).
[48] R. Kubo, Rep. Prog. Phys. **29**, 255 (1966).
[49] L. Arnold, *Random Dynamical Systems* (Springer, Berlin, 1998).
[50] M. Abramowitz and I. A. Stegun, *Pocketbook of Mathematical Functions* (Verlag Harri Deutsch, Frankfurt/Main, 1984).
[51] R. F. Grote and J. T. Hynes, J. Chem. Phys. **73**, 2715 (1980).
[52] D. V. Widder, *The Laplace Transform* (Princeton University Press, Princeton, 1946).